

Crystal Engineering Using Anilic Acids and Dipyridyl Compounds through a New Supramolecular Synthron

Md. Badruz Zaman,^{†,‡} Masaaki Tomura,^{*,†} and Yoshiro Yamashita^{*,§}

Institute for Molecular Science, Myodaiji, Okazaki 444-8585, Japan, and Department of Electronic Chemistry, Interdisciplinary Graduate School of Science and Engineering, Tokyo Institute of Technology, 4259 Nagatsuta, Midori-ku, Yokohama 226-8502, Japan

yoshiro@echem.titech.ac.jp

Received December 14, 2000

The anilic acids, 2,5-dihydroxy-1,4-benzoquinone (**1a**), 2,5-dibromo-3,6-dihydroxy-1,4-benzoquinone (bromanilic acid; **1b**), 2,5-dichloro-3,6-dihydroxy-1,4-benzoquinone (chloranilic acid; **1c**), and 2,5-dicyano-3,6-dihydroxy-1,4-benzoquinone (cyananilic acid; **1d**), were cocrystallized with rigid organic ligands containing two pyridine rings, 2,4-bipyridine (**2a**), 4,4'-bipyridine (**2b**), 1,2-bis(2-pyridyl)-ethylene (**3a**), 1,2-bis(4-pyridyl)ethylene (**3b**), 2,2'-dipyridylacetylene (**4a**), 3,3'-dipyridylacetylene (**4b**), and 4,4'-dipyridylacetylene (**4c**). Fourteen complexes **5–18** were obtained as single crystals, and their crystal structures were successfully determined by X-ray analysis. All complexes except those with **2a** are 1:1 and are composed of an infinite linear or zigzag tape structure, the formation of which is ascribed to intermolecular O–H···N, N⁺–H···O, or N⁺–H···O[–] hydrogen bonds or a combination of these between the anilic acids and the dipyridyl compounds. In the complexes **5** and **6**, no infinite tape structure is observed although the molecular units connected by a similar hydrogen-bonding pattern are formed. For the 1:1 complexes, we have found two types of stacking arrangements, segregated stacks (**7**, **9**, **12–15**, **18**) and alternated ones (**8**, **10**, **11**, **16**, **17**). In the complexes of **1c** with the series of dipyridylacetylenes **4** (**14**, **15**, **17**), the neutral, dication, and monocation states are formed depending on the nitrogen positions, which can be attributed to the different basicity of the pyridyl groups.

Introduction

Organic solid materials based on hydrogen-bonded donor and acceptor molecules have been the objects of recent intensive studies¹ aimed at building a new class of compounds which are interesting from viewpoints of basic science as well as of applications such as biological sensors and catalysis.^{2–5} Hydrogen bonding is expected to regulate electronic properties of solids and work as switching units for molecular devices. Rational design

based on crystal engineering^{2–4} including supramolecular chemistry⁵ is particularly important for the progress of this field. This is considered to be accomplished by fundamental studies on weak intermolecular interactions which govern orientation, recognition, and assembly of components in the solid state. Specific noncovalent interactions between different functionalities seem to control single and multicomponent crystallization.

Our work has focused on the development of new organic donor–acceptor (DA) interactions as supramo-

* To whom correspondence should be addressed. Phone: +81-45-924-5571. Fax: +81-45-924-5489.

[†] Institute for Molecular Science.

[‡] Permanent address: Department of Applied Chemistry and Chemical Technology, University of Dhaka, Dhaka-1000, Bangladesh.

[§] Tokyo Institute of Technology.

(1) Some reviews for hydrogen-bond donor and acceptor molecules: (a) Kyugoku, Y.; Lord, R. C.; Rich, A. *Proc. Natl. Acad. Sci. U.S.A.* **1967**, *57*, 250. (b) Martin, T. W.; Derewenda, Z. S. *Nat. Struct. Biol.* **1999**, *6*, 403. (c) Melendez, R. E.; Carr, A. J.; Linton, B. R.; Hamilton, A. W. In *Molecular Self-Assembly Organic Versus Inorganic Approaches*; Fujita, M., Ed.; Structure and Bonding, Vol. 96; Springer-Verlag: Berlin and Heidelberg, Germany, 2000; p 31. (d) Zimmerman, S. C.; Corbin, P. S. In *Molecular Self-Assembly Organic Versus Inorganic Approaches*; Fujita, M., Ed.; Structure and Bonding, Vol. 96; Springer-Verlag: Berlin and Heidelberg, Germany, 2000; p 63. (e) Jeffrey, G. A. *An Introduction to Hydrogen Bonding*; Oxford University Press: Oxford, U.K., 1997.

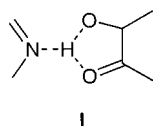
(2) (a) Mitani, T. *Mol. Cryst. Liq. Cryst.* **1989**, *171*, 343. (b) Gokel, G. W. *Chem. Soc. Rev.* **1992**, *21*, 39. (c) Izatt, R. M.; Bruening, R. L.; Tarbet, B. J.; Griffin, L. D.; Bruening, M. L.; Karkowiak, K. E.; Bradshaw, J. S. *Pure Appl. Chem.* **1990**, *62*, 1115. (d) McGrady, J. E.; Stranger, R. *J. Am. Chem. Soc.* **1997**, *119*, 8512. (e) Casades, I.; Fornes, V.; Gigante, B.; Garcia, H. *Chem. Phys. Lett.* **1999**, *305*, 365. (f) Chenthamarakshan, C. R.; Eldo, J.; Ajayaghosh, A. *Macromolecules* **1999**, *32*, 251. (g) Hulliger, J.; Langley, P. J.; Quintel, A.; Rechsteiner, P.; Roth, S. W. In *Supramolecular Engineering of Synthetic Metallic Materials*; Veciana, J.; Rovira, C.; Amabilina, D. B., Eds.; NATO ASI Series C, Kluwer: London, 1999; p 67.

(3) For an overview of recent crystal engineering, see the following volumes: (a) *Comprehensive Supramolecular Chemistry*; Atwood, J. L.; Davies, J. E. D.; MacNicol, D. D.; Vogtle, F.; Lehn, J.-M., Eds.; Pergamon: Oxford, U.K., 1996; Vol. 6. (b) *Crystal Engineering: The Design and Applications of Functional Solids*; Seddon, K. R.; Zaworotko, M. J., Eds.; NATO ASI Series; Kluwer Academic: Dordrecht, The Netherlands, 1998. (c) *Design of Organic Solids*; Weber, E., Ed.; Topics in Current Chemistry; Springer-Verlag: Berlin and Heidelberg, Germany, 1998; Vol. 198. (d) *Crystal Engineering: From Molecules and Crystals to Materials*; Braga, D.; Grepioni, F.; Orpen, A. G., Eds.; NATO ASI Series C; Kluwer Academic: Dordrecht, The Netherlands, 1999. (e) *Molecular Self-Assembly Organic Versus Inorganic Approaches*; Fujita, M., Ed.; Structure and Bonding; Springer-Verlag: Berlin and Heidelberg, Germany, 2000; Vol. 96.

(4) Some crystal engineering reviews are: (a) Desiraju, G. R. *Crystal Engineering: The Design of Organic Solids*; Elsevier: Amsterdam, 1989. (b) Etter, M. C. *Acc. Chem. Res.* **1990**, *23*, 120. (c) Etter, M. C.; Urbanczyk-Lipkowska, Z.; Zia-Ebrahimi, M.; Panunto, T. W. *J. Am. Chem. Soc.* **1990**, *112*, 8415. (d) Zhao, X.; Chang, Y.-L.; Fowler, F. W.; Lauher, J. W. *J. Am. Chem. Soc.* **1990**, *112*, 6627. (e) Aakeroy, C. B.; Seddon, K. R. *Chem. Soc. Rev.* **1993**, 397. (f) Chang, Y.-L.; West, M.-A.; Fowler, F. W.; Lauher, J. W. *J. Am. Chem. Soc.* **1993**, *115*, 5991. (g) MacDonald, J. C.; Whitesides, G. M. *Chem. Rev.* **1994**, *94*, 2383. (h) Subramaniam, S.; Zaworotko, M. *Coord. Chem. Rev.* **1994**, *137*, 354. (i) Russel, V. A.; Ward, M. D. *Chem. Mater.* **1996**, *8*, 1654. (j) Aakeroy, C. B. *Acta Crystallogr., Sect. B* **1997**, *53*, 569. (k) Desiraju, G. R. *Angew. Chem., Int. Ed. Engl.* **1995**, *34*, 2311. (l) Hosseini, M. W.; André, D. C. *Chem. Commun.* **1998**, 727. (m) Brammer, L.; Zhao, D.; Ladipo, F. T.; Braddock-Wilking, J. *Acta Crystallogr., Sect. B* **1995**, *51*, 632.

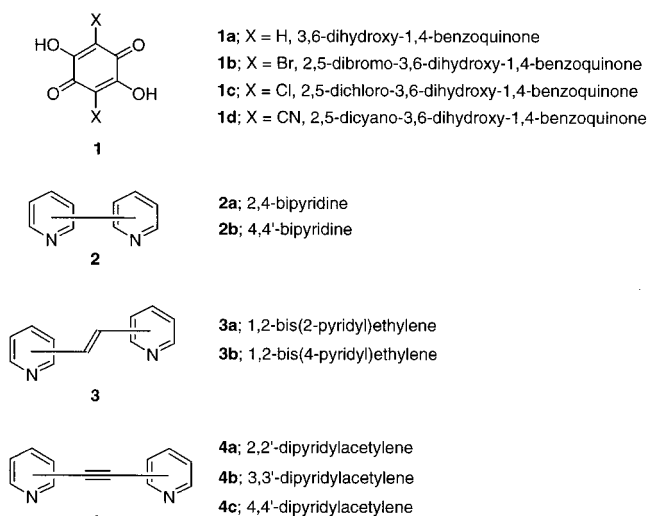
lecular synthons for the preparation of ordered solid phases.⁶ Our strategy is to investigate geometrically and stoichiometrically matched donor and acceptor molecules which can be used to propagate oriented patterns in the crystal engineering. We are concerned with the use of organic component molecules which can form a variety of structures and mediate electron–proton transfer. Employing organic molecules to form crystalline architectures seems an attractive idea for a crystal engineering approach. Simple association of two complementary compounds through noncovalent interactions can be used to create organic materials with new remarkable physical properties and potential applications in optical and electronic devices, which are not possessed by either of the components alone.^{2e–g,13}

Our attempt is to develop a new tool for crystal engineering that is associated with a great variety of hydrogen-bonded DA-type compounds in which donor and acceptor molecules can be combined within robust hydrogen-bonded architectures. Development of new supramolecular synthons with specific bonding features is important to design materials with interesting features. We have chosen benzoquinone-type molecules with dihydroxy groups, anilic acids, which have excellent proton-donating properties and can undergo multistage deprotonation and protonation processes. These acids can be associated with a variety of proton acceptors as counterpart to give predictable supramolecular architectures. In the course of this work, we have prepared cyananilic acid (**1d**)⁷ as a poor electron acceptor molecule and studied it as a hydrogen-bonded counterion in conducting charge-transfer complexes with a variety of organic sulfur-containing donors.^{8,9} The monoanion and dianion of **1d** were assembled into supramolecular structures through the one- and two-dimensional hydrogen-bonded network.¹⁰ In our preliminary communication, we have used dipyrindyl-type bases as proton acceptors and constructed a new supramolecular synthon (**I**) motif.¹¹ We have also



prepared three rigid organic ligands containing pyridine

Scheme 1



Crystalline Complexes

- | | |
|---|---|
| 5 ; complex between 1b and 2a | 12 ; complex between 1a and 4c |
| 6 ; complex between 1c and 2a | 13 ; complex between 1b and 4a |
| 7 ; complex between 1a and 2b | 14 ; complex between 1c and 4a |
| 8 ; complex between 1c and 2b | 15 ; complex between 1c and 4b |
| 9 ; complex between 1c and 3a | 16 ; complex between 1b and 4c |
| 10 ; complex between 1b and 3b | 17 ; complex between 1c and 4c |
| 11 ; complex between 1c and 3b | 18 ; complex between 1d and 4c |

rings separated by an acetylene spacer (**4a–c**) that formed crystalline complexes with a common organic acid (**1c**).¹² These complexes have infinite one-dimensional tapelike structures that lead to supramolecular polymeric systems. As a continuation of these works, we have attempted to combine a variety of proton donor and acceptor molecules to obtain novel supramolecular structures. In this paper, we will present the preparation of supramolecular complexes by complementary combination of proton donors (D) (anilic acids, **1**) and proton acceptors (A) (bidentate nitrogen ligands, **2–4**) via hydrogen-bonded interactions (Scheme 1).

Results

Preparation of Cocrystals. Generally, the formation of cocrystals of proton donors (D) and acceptors (A) requires the following conditions: (i) D and A molecules matched geometrically and stoichiometrically, (ii) facile acid–base reactions between D and A molecules, (iii) good solubility of the D and A molecules in solvents, and (iv) precipitation of the formed complexes from the solution. Considering the above conditions, we have successfully obtained single crystals of complexes **5–18** composed of anilic acids and dipyrindyl compounds. The following three simple procedures were used to obtain the above single crystals suitable for X-ray analysis: (i) slow diffusion using an H-shaped tube, (ii) mixing of two components in hot solutions, and (iii) slow evaporation technique. Methanol, ethanol, acetone, acetonitrile, and their mixture in various ratios were used as solvents for the preparation of these cocrystals. Details of the synthesis are explained in the Experimental Section.

Structural Analyses. The cocrystals of anilic acids with dipyrindyl compounds obtained here take various

- (5) (a) Lehn, J.-M. *Supramolecular Chemistry*; VCH: Weinheim, Germany, 1995. (b) *Comprehensive Supramolecular Chemistry*; Atwood, J. L.; Davies, J. E. D.; MacNicol, D. D.; Vogtle, F.; Lehn, J.-M., Eds.; Pergamon: Oxford, U.K., 1996; Vols. 1–11.
- (6) (a) Greer, M. L.; Blackstock, S. C. *J. Org. Chem.* **1996**, *61*, 7895. (b) Blackstock, S. C.; Poehling, K.; Greer, M. L. *J. Am. Chem. Soc.* **1995**, *117*, 6617. (c) Greer, M. L.; McGee, B. J.; Rogers, R. D.; Blackstock, S. C. *Angew. Chem., Int. Ed. Engl.* **1997**, *36*, 1864. (d) McGee, B. J.; Sherwood, L. J.; Greer, M. L.; Blackstock, S. C. *Org. Lett.* **2000**, *2*, 1180.
- (7) (a) Wallenfels, K.; Bachmann, G.; Hofmann, D.; Kern, R. *Tetrahedron* **1965**, *21*, 2239. (b) Zaman, M. B.; Morita, Y.; Toyoda, J.; Yamochi, H.; Sekizaki, S.; Nakasuji, K. *Mol. Cryst. Liq. Cryst.* **1996**, *187*, 249.
- (8) Zaman, M. B.; Morita, Y.; Toyoda, J.; Yamochi, H.; Saito, G.; Yoneyama, N.; Enoki, T.; Nakasuji, K. *Chem. Lett.* **1997**, 729.
- (9) Zaman, M. B.; Toyoda, J.; Morita, Y.; Yamochi, H.; Saito, G.; Nakasuji, K. *Synth. Met.* **1999**, *102*, 1691.
- (10) Yamochi, H.; Nakamura, S.; Saito, G.; Zaman, M. B.; Toyoda, J.; Morita, Y.; Nakasuji, K.; Yamashita, Y. *Synth. Met.* **1999**, *102*, 1729.
- (11) Zaman, M. B.; Tomura, M.; Yamashita, Y. *Chem. Commun.* **1999**, 999.
- (12) Zaman, M. B.; Tomura, M.; Yamashita, Y. *Org. Lett.* **2000**, *2*, 273.
- (13) (a) MacGillivray, L. R.; Spinney, H. A.; Reid, J. L.; Ripmester, J. A. *Chem. Commun.* **2000**, 517. (b) Batchelor, E.; Klinowski, J.; Jones, W. J. *Mater. Chem.* **2000**, *10*, 839.

structures which were clarified by X-ray analysis. To rationally control the structures, we have examined the effects of the spacers and nitrogen positions in the dipyrindyl compounds and substituents (H, Br, Cl, CN) of the anilic acid that influence the solubility, hydrogen-bonding ability, ionicity, geometry, and stacking arrangements of the molecules. The structures of the 14 complexes are discussed below. The geometry of the intermolecular hydrogen bonds for the complexes for which X-ray structures are first determined in this paper is summarized in Table 1.

Complexes 5 and 6. The complexes are isomorphous and crystallize in the monoclinic $P2_1/n$ space group, and the molecules **1b** in **5** and **1c** in **6** are located on the inversion center. The complexes have a 1:2 (D/A) stoichiometric ratio with the transfer of the two acidic protons of the donors to the nitrogen atoms of the acceptors to give a monoprotinated cation. The hydrogen atom positions in these cocrystals were identified on different Fourier maps and further confirmed by careful observation of C–O bond lengths and concerned hydrogen-bonding distances. The nitrogen atoms at the 4-position of the pyridine rings form a bifurcated interionic $N^+ \cdots H \cdots O^-$ (1.71 Å for **5** and 1.74 Å for **6**) and $N^+ \cdots H \cdots O$ (2.29 Å for **5** and **6**) hydrogen-bonded network (see Table 1). Thus, the robust synthon **I** generated at the 4-position forms molecular $A \cdots D \cdots A$ -type pairs. The views of such crystalline architecture and their synthon **I** are shown in Figure 1. There is no hydrogen-bonding interaction in the nitrogen atom at the 2-position of the pyridine ring, and as a consequence, no infinite $(D \cdots A)_n$ linkage was observed, in contrast to the structures of 1:1 complexes described below. Moreover, the pyridine rings are twisted at the central C–C bond with a dihedral angle of 16.4° for **5** and 15.4° for **6** between the ring planes. Therefore, the nitrogen atom at the 2-position of the pyridine ring is diverted much closer to the adjacent hydrogen-bonded $A \cdots D \cdots A$ pairs, where the distances between the planes of **1b,c** and **2a** within the DA pair are 3.42 Å for **5** and 3.40 Å for **6**. The distances between the planes of the 2-pyridine rings (3.43 Å for **5** and 3.40 Å for **6**) suggest closer AA interactions in the adjacent hydrogen-bonded $A \cdots D \cdots A$ pairs. Thus, a pair of $A \cdots D \cdots A$ aggregation is close-packed in alternated stacking arrangements with other pairs from the DA- or AA-type connectivity (Figure 2).

Complex 7. The complex crystallizes in the monoclinic $C2/c$ space group, and both **1a** and **2b** are located on the inversion center. The geometry and the C=O, C–OH, and C–C bond distances are consistent with those of the typical neutral anilic acids.¹⁴ In this complex, no proton is transferred from the acid to the base molecule. However, intermolecular hydrogen-bonded $H-O \cdots N$ and $=O \cdots N$ distances of 2.63 and 3.08 Å are observed (Figure 3), which create the robust supramolecular synthon **I**. The **1a** and **2b** units are linked by $O-H \cdots N$ hydrogen bonds (1.55 Å) into a one-dimensional infinite molecular tape along the [1 0 2] direction. The angle between the two pyridine rings in **2b** is 29.2°, and two molecules of

Table 1. Geometry of the Intermolecular Hydrogen Bonds between the Anilic Acids and the Dipyrindyl Compounds in the Complexes **5–7**, **10–13**, **16**, and **18**

complex		distance ^a (Å)				angle ^b (deg)
		D–H \cdots A	D–H	H \cdots A	D \cdots A	D–H \cdots A
5^c	N2–H2A \cdots O2 ⁱ	0.99(4)	1.71(4)	2.635(3)	155(3)	
	N2–H2A \cdots O1 ⁱⁱ	0.99(4)	2.29(4)	2.951(3)	123(3)	
6^c	N2–H2 \cdots O2 ⁱⁱⁱ	0.96(3)	1.74(3)	2.621(2)	151(3)	
	N2–H2 \cdots O2 ⁱⁱⁱ	0.96(3)	2.29(3)	2.969(3)	127(2)	
7	O1–H1 \cdots N1	1.15(6)	1.55(6)	2.641(6)	157(5)	
10^c	N1–H1 \cdots O1 ^{iv}	0.95(8)	1.71(8)	2.644(4)	167(8)	
	N1–H1 \cdots O2 ^{iv}	0.95(8)	2.53(8)	3.077(4)	117(6)	
11	N1–H1 \cdots O1	1.01(6)	1.66(6)	2.641(4)	164(5)	
	N1–H1 \cdots O2	1.01(6)	2.49(6)	3.044(5)	114(4)	
12	O1–H1 \cdots N1	1.07(5)	1.70(4)	2.654(3)	146(4)	
13^c	O2–H2A \cdots N1 ^v	1.18(10)	1.59(10)	2.642(3)	145(8)	
16^c	N1–H1 \cdots O4 ^{vi}	1.04(6)	1.58(6)	2.577(4)	158(5)	
	N1–H1 \cdots O3 ^{vi}	1.04(6)	2.34(5)	2.971(5)	118(4)	
18^c	O2–H2A \cdots N2 ^{vii}	1.21(9)	1.43(9)	2.617(4)	164(7)	
	N1–H1 \cdots O1 ^{viii}	0.86(2)	2.01(5)	2.738(8)	142(6)	
	N1–H1 \cdots O2	0.86(2)	2.22(5)	2.927(9)	140(6)	

^a A hydrogen bond for which the H \cdots A distance is below the sum of the covalent radius of A and 2.0 Å is listed. ^b A hydrogen bond for which D–H \cdots A angle is above 110° is listed. ^c Symmetry code *i*: $x + 3/2, -y + 3/2, z - 1/2$. *ii*: $-x + 3/2, y - 1/2, -z + 3/2$. *iii*: $x + 3/2, -y + 1/2, z - 1/2$. *iv*: $-x + 2, y + 1/2, -z + 3/2$. *v*: $x, y + 1, z - 1$. *vi*: $x - 1/2, -y + 1/2, z - 1/2$. *vii*: $x + 1/2, -y + 1/2, z - 1/2$. *viii*: $-x + 1, -y + 1, -z$.

1a in the tapes tilt toward the pyridine rings with the angles of 19.6° and 48.6°. Each molecule in the tapes forms a segregated stacking along the [0 1 1] direction (Figure 4).

Complex 8. The complex crystallizes in the monoclinic $P2_1/n$ space group, and both **1c** and **2b** are located on the inversion center. In this complex, both of the hydroxyl protons are transferred from **1c** to the nitrogen atoms of the pyridine rings of **2b**, and attractive one-dimensional infinite molecular tape structures are formed through the robust supramolecular synthon **I**. Details of the crystalline architecture are described in our preliminary communication.¹¹ The C–O bond distances are shorter than those found in other dianion structures. The ring C–C bond distances are also consistent with those of the dianion with an aromatic ring.¹⁴

Complex 9. The complex crystallizes in the triclinic $P\bar{1}$ space group, and both **1c** and **3a** are located on the inversion center. In the complex **9**, the dianion of **1c** is observed and the dianion has similar C–O and C–C bond distances to those in the complex **8**.^{11,14} The central C=C bond length [1.313(5) Å] of **3a** is a typical value of a double bond, and the configuration around the double bond is trans. The crystal architecture, stacking arrangement, and hydrogen-bonded linkage through the supramolecular synthon **I** are previously described and will not be discussed again.¹¹

Complexes 10 and 11. The complexes are isomorphous and crystallize in the monoclinic $P2_1/c$ space group, and **1b,c** and **3b** are located on the inversion center. Both of the acids **1b**¹⁵ and **1c**^{14,15} are fully deprotonated to produce the dianions. These structures also involve bifurcated $N^+ \cdots H \cdots O$ hydrogen bonds (2.64 and 3.08 Å for **10**, 2.64 and 3.04 Å for **11**) between the nitrogen atoms of **3b** and the two oxygen atoms of **1b,c**, thus

(14) (a) Andersen, E. K. *Acta Crystallogr.* **1967**, *22*, 188. (b) Andersen, E. K. *Acta Crystallogr.* **1967**, *22*, 191. (c) Andersen, E. K. *Acta Crystallogr.* **1967**, *22*, 196. (d) Bencheikroun, R.; Savariault, J.-M. *Acta Crystallogr., Sect. C* **1995**, *51*, 186. (e) Kanters, J. A.; Schouten, A.; Duisenberg, A. J. M.; Glowiak, T.; Malarski, Z.; Sobczyk, L.; Greach, E. *Acta Crystallogr., Sect. C* **1991**, *47*, 2148. (f) Zaman, M. B.; Tomura, M.; Yamashita, Y.; Sayaduzzaman, M.; Chowdhury, A. M. S. *CrysoEngComm* **1999**, *9*.

(15) (a) Robl, C. *Mater. Res. Bull.* **1987**, *22*, 1483. (b) Robl, C.; Weiss, A. *Mater. Res. Bull.* **1987**, *22*, 497. (c) Aliev, A. G.; Kondrat'ev, S. I.; Atovmyan, L. O.; Karpov, V. V. *Bull. Acad. Sci. USSR* **1981**, *30*, 339.

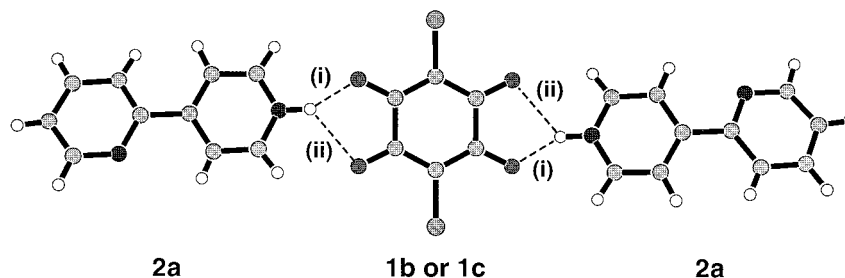


Figure 1. Hydrogen-bonded A...D...A pair of **5** and **6**. Dotted lines show the intermolecular N–H...O hydrogen bonds: (i) 1.71 Å for **5** and 1.74 Å for **6**; (ii) 2.29 Å for **5** and **6**.

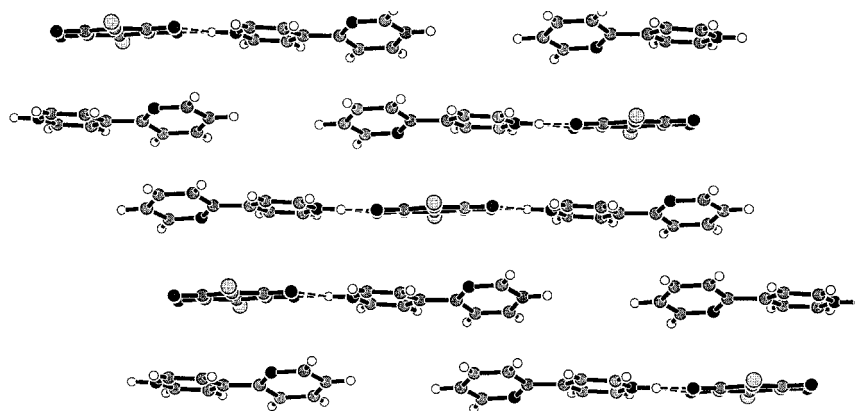


Figure 2. Alternated stacking arrangements of **6**, which contain pyridine rings–bromanilate rings and pyridine rings–pyridine rings overlaps. Dotted lines show the intermolecular N–H...O hydrogen bonds.

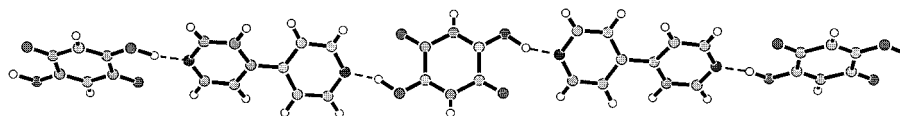


Figure 3. One-dimensional molecular tape of **7**. Dotted lines show the intermolecular O–H...N hydrogen bonds (1.55 Å).

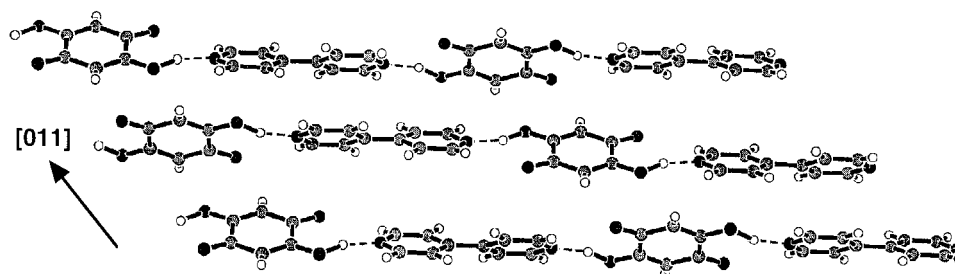


Figure 4. Segregated stacking arrangements along the [0 1 1] direction of **7**. Dotted lines show the intermolecular O–H...N hydrogen bonds.

creating the robust supramolecular synthon **I**. In both **10** and **11**, one-dimensional molecular tape structures are observed toward the two cross diagonal lines within the *ab* plane. The crossed tape structures are shown in Figure 5. Within the tape structures, the dihedral angles between the planes of **1b,c** and the pyridine rings are 24.2° and 23.5° for **10** and **11**, respectively. The molecular tapes in **10** and **11** run in a mild zigzag fashion because of the trans configuration of **3b**. Moreover, the molecules **1b,c** and **3b** in **10** and **11** compose alternated stacks along the [1 1 0] and [−1 1 0] directions (Figure 6). The DA pair in the alternated stacking involves close contacts between the adjacent tapes, where the distances between the planes of **1b,c** and **3b** are 3.55 and 3.53 Å for **10** and **11**, respectively.

Complex 12. The complex crystallizes in the monoclinic $P2_1/n$ space group, and both **1a** and **4c** are located on the inversion center. The bond distances and the angles of **1a** in **12** are similar to those in the complex **7**. Two molecules, **1a** and **4c**, connect with an intermolecular O–H...N hydrogen bonding (2.65 Å), and the dihedral angle between the planes of the pyridine ring of **4c** and **1a** is 4.5°. No proton transfer from **1a** to **4c** is observed. An infinite one-dimensional tape structure with an intertape distance of 3.4 Å is formed along the [2 0 1] direction. In addition, each component molecule forms a segregated stacking along the *a* axis (Figure 7).

Complexes 13 and 14. The complexes are isomorphous and crystallize in the triclinic $P\bar{1}$ space group, and both **4a** and **1b,c** are located on the inversion center. The

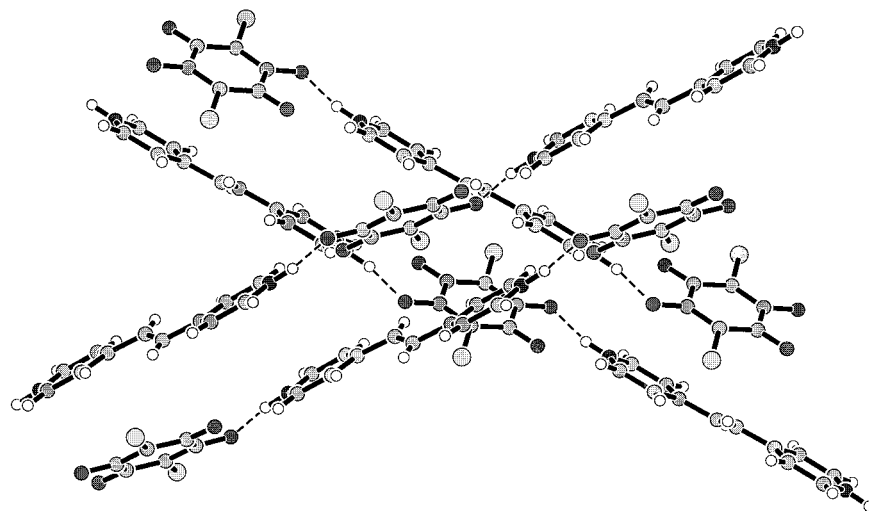


Figure 5. Two crossed one-dimensional molecular tapes of **10**. Dotted lines show the intermolecular N–H···O hydrogen bonds.

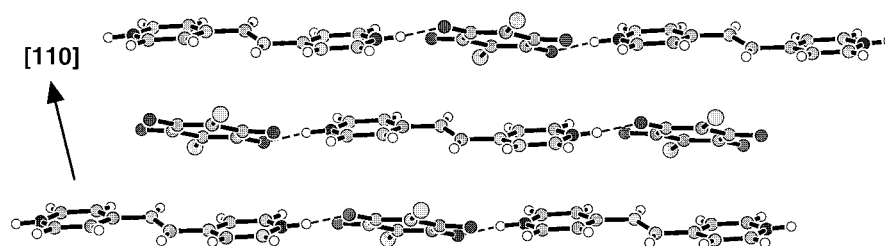


Figure 6. Alternated stacking arrangements along the [1 1 0] direction of **10**. Dotted lines show the intermolecular N–H···O hydrogen bonds.

molecular structure and stacking arrangements of the complex **13** are similar to those of the complex **14**, which was previously reported.¹² No proton transfer from **1b,c** to **4a** is observed. These complexes contain a zigzag one-dimensional tape structure with an infinite linkage of **1b,c** and **4a** through the supramolecular synthon **I** and have segregated stackings with DD- and AA-type pairs.

Complex 15. The complex crystallizes in the triclinic $P\bar{1}$ space group, and both **1c** and **4b** are located on the inversion center. The complex **15** contains 3.3 molecules of water. Both of the protons transfer from the hydroxyl groups of **1c** to the nitrogen atoms of **4b**. Thus, the two molecules, **1c** and **4b**, connect with interionic $N^+ - H \cdots O^-$ (2.65 Å) and $N^+ - H \cdots O =$ (2.87 Å) hydrogen bonds and form the supramolecular synthon **I**. The molecular architecture displays a zigzag tape structure, which is viewed as a square grid-type network along the *c* axis (Figure 8). Within the network, cavities are formed, which are occupied by the water molecules. Each component molecule forms a segregated stacking along the *c* axis. Details of this interesting structure are described in our preliminary communication.¹²

Complexes 16 and 17. The complexes are isomorphous and crystallize in the monoclinic $P2_1/n$ space group, and both **1b,c** and **4c** are located on a general position. The molecular structure and stacking arrangements of the complex **16** are similar to those of the complex **17**, which was previously reported.¹² In the crystal structure of **16**, one pyridine ring of **4c** is protonated and combines with **1b** via bifurcated $N^+ - H \cdots O^-$ (2.58 Å) and $N^+ - H \cdots O =$ (2.97 Å) hydrogen bonds, while the other pyridine ring is not protonated and forms $H - O \cdots N$ (2.62 Å) and $=O \cdots N$ (2.98 Å) hydrogen-bonding interactions (see Table

1). Thus, an infinite one-dimensional molecular tape structure is observed along the *c* axis (Figure 9). Two pyridine rings of **4c** in **16** are twisted with dihedral angles of 78.0°. In this work, **16** and **17** are the only examples of complexes containing a dipyrindyl compound with two perpendicular pyridine rings. The dihedral angles between the planes of **1b** and the pyridine rings of **4c** are 73.5° and 4.5° for the nonprotonated and protonated side, respectively. The component molecule **1b** is partially overlapped with the protonated pyridine ring of **4c** and forms an alternated DA-type stacking along the *b* axis with **4c**.

Complex 18. The complex crystallizes in the triclinic $P\bar{1}$ space group, and both **1d** and **4c** are located on the inversion center. The geometry of **1d** has similar C–O and C–C bond distances to those of our previously described complexes of **1d**.^{9,16} The component molecules **1d** and **4c** connect via the bifurcated $N^+ - H \cdots O^-$ and $N^+ - H \cdots O$ hydrogen bonds ($N \cdots O$ distances, 2.74 and 2.93 Å) and form the robust supramolecular synthon **I**. This is the first example of the supramolecular synthon **I** with **1d**. Thus, an infinite one-dimensional tape structure along the [1 1 0] direction is observed. The intertape distances, which are 3.22 and 3.42 Å for the distances between **1d**–**1d** and **4c**–**4c** planes, respectively, are very close. The dihedral angle between the plane of **1d** and the pyridine ring of **4c** is 59.6°. The most remarkable feature of the molecular tape in **18** is its bent structure with the angle of 121° at the hydrogen-bonding coupling part of the tape. This value is unusual compared to the

(16) Andersen, E. K.; Andersen, I. G. K. *Acta Crystallogr., Sect. B* 1975, 31, 379.

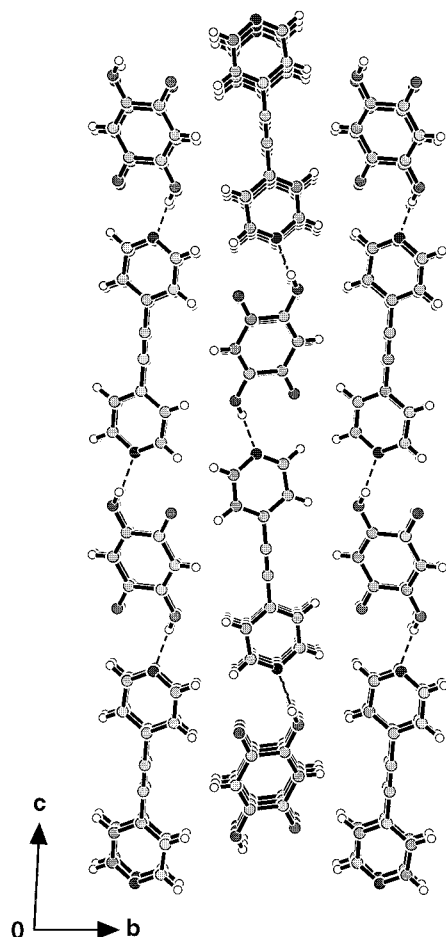


Figure 7. Packing diagram of **12** viewed along the *a* axis. One-dimensional molecular tape is formed along the [2 0 1] direction. Dotted lines show the intermolecular O–H...N hydrogen bonds (2.65 Å), and the C=O...N interaction is 3.04 Å.

other molecular tape structures described in this work (the corresponding angles for the tape structures of the complexes **7**, **10–14**, and **16** are 155°–178° with an average of 170°). Such features of the tape structure in **18** are illustrated in Figure 10. Each component molecule forms a segregated DD- and AA-type stacking along the *c* axis (Figure 11).

Discussion

We discuss here the factors determining the crystal structures described above. The structures of these complexes are related to the following factors: (i) the positions of the nitrogen atoms of the dipyridyl compounds, (ii) the proton-donating abilities of the anilic acids which are determined by the substituents, and (iii) the geometry of the one-dimensional molecular tape structures.

The donor–acceptor ratios of the complexes **5** and **6** are 1:2, while the other complexes **7–18** have 1:1 composition. The 1:2 complexes are obtained from only 2,4-bipyridine, while the 1:1 complexes are derived from the symmetrical dipyridyl compounds. In the 1:2 complexes, the hydrogen bond is formed at the 4-pyridyl ring and the nitrogen of the 2-pyridyl ring is not involved in the hydrogen bonding. This fact can be explained by the difference in the basicity of the pyridine rings depending

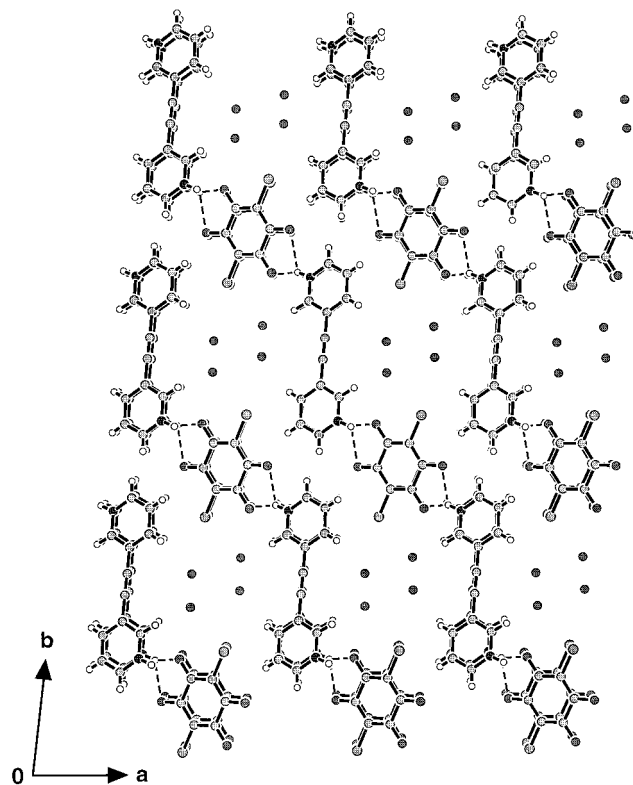


Figure 8. Square grid-type network of **15** viewed along the *c* axis. The cavities are occupied by the water molecules. Dotted lines show the intermolecular N–H...O hydrogen bonds.

on the nitrogen positions. The PM3 calculations¹⁷ show that the net atomic charges of the nitrogen atoms of 4- and 2-pyridyl rings in 2,4-bipyridine are –0.0719 and –0.0668, respectively, suggesting that the basicity is higher at the 4-position than it is at the 2-position.

In the 1:1 complexes, linear and zigzag molecular tape structures are observed. The linear tape structures are obtained only from the 4,4'-dipyridyl derivatives. On the other hand, the 2,2'- and 3,3'-isomers bring the zigzag tape structures. The 3,3'-isomer particularly gives a unique grid-like structure with a void. In the case of the complex **18**, the zigzag tape structure is produced despite the 4,4'-isomer **4c** in **18**. Compared with other zigzag tape structures, the zigzag tape in **18** bends at the coupling part via intermolecular hydrogen bonds or at the supramolecular synthon **I**. Such a conformation of the tape causes close packing of the tapes and stabilizes the crystal structure. It is noteworthy that the linear tape structures appear in the monoclinic crystal system and the triclinic crystal system affords zigzag tapes.

The positions of nitrogen atoms of the pyridyl groups also affect the ionicity of the complexes. In the complexes of **1c** with dipyridylacetylene **4** (complexes **14**, **15**, and **17**), the neutral (from the 2,2'-derivative **4a**), dication (from the 3,3'-derivative **4b**), and monocation (from the 4,4'-derivative **4c**) states are observed. Although molecular packing and morphology in the solid state may affect the proton transfer to the nitrogen atoms of the pyridyl groups, the major reasons for these phenomena can be attributed to the differences in the basicity of the pyridyl groups depending on the nitrogen positions.¹² This is

(17) (a) Stewart, J. J. P. *J. Comput. Chem.* **1989**, *10*, 209. (b) Stewart, J. J. P. *J. Comput. Chem.* **1989**, *10*, 221.

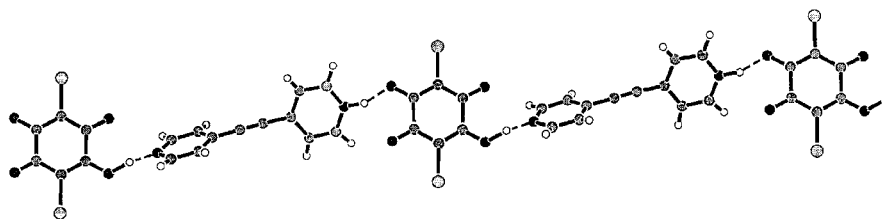


Figure 9. One-dimensional molecular tape of **16**. Dotted lines show two types of the intermolecular hydrogen bonds, $N^+-H\cdots O$ (1.58 Å) and $O-H\cdots N$ (1.43 Å).

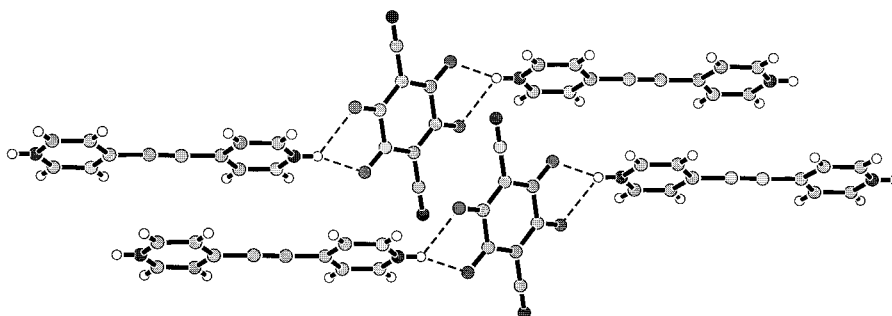


Figure 10. Two one-dimensional molecular tapes of **18**. Dotted lines show the intermolecular $N^+-H\cdots O$ hydrogen bonds (2.01 and 2.22 Å).

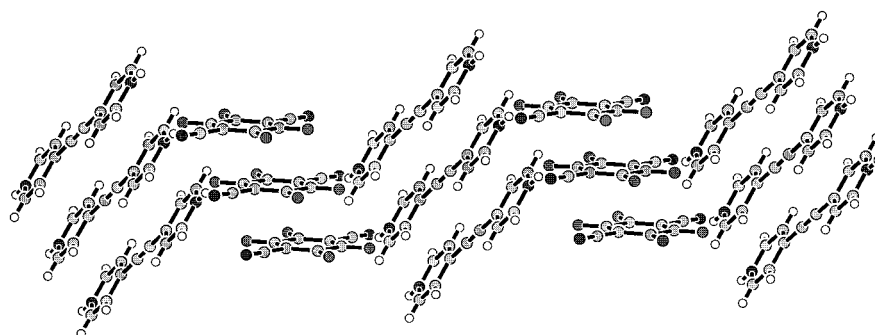


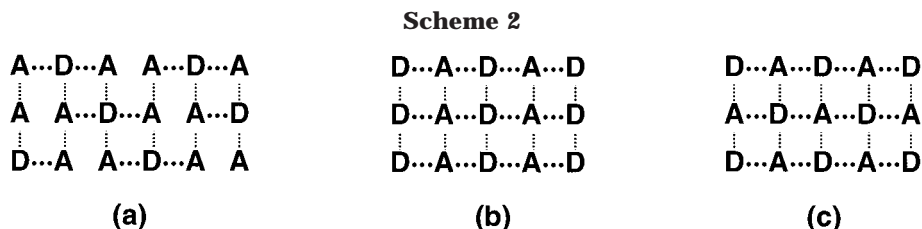
Figure 11. Segregated stacking arrangements along the *c* axis of **18**. The interstack distances are 3.22 and 3.42 Å for the stacks of **1d** and **4c**, respectively.

supported by the PM3 calculations of the net atomic charge of the nitrogen atoms of **4** (**4a**, -0.0607 ; **4b**, -0.0771 ; **4c**, -0.0742).

Among the four anilic acids used in this work, **1a** has the lowest proton-donating property, and the crystalline complexes **7** and **12** obtained from **1a** are neutral. Acids **1b** and **1c** with moderate proton-donating ability afford monoprotonated or deprotonated complexes with dipyrindyl compounds containing nitrogen atoms at the 4- or 3-position of the pyridine rings. These acids form neutral complexes **13** and **14** with the weakest proton-accepting base **4a** containing nitrogen atoms at the 2-position of the pyridine rings. Only the crystalline complex **18** obtained from the strongest proton donor **1d** with **4c** is fully deprotonated and involves relatively short contacts between the neighboring donor and acceptor molecules. The acid **1d** rapidly produces colored powders with other dipyrindyl compounds **2–4**, even if polar solvents are used for the preparation of complexes. The rapid complexation of **1d** is attributed to its strong proton-donating ability.

For the rational design of supramolecular architectures, strategies with structural predictability can be used in the construction of one-, two-, or three-dimensional patterns. A primary one-dimensional tape motif can be designed and obtained by using strong intermo-

lecular interactions such as hydrogen bonding. The addition of functional groups or weaker intermolecular interactions to the tapes can expand the one-dimensional networks into two-dimensional layers or sheets. A three-dimensional supramolecular architecture can be achieved by the same process to connect the two-dimensional layers. In this study, we have found three types of stacking arrangements, the patterns of which are illustrated in Scheme 2. In the complexes **5** and **6**, the $A\cdots D\cdots A$ units overlap two-dimensionally to form a cross-linked layer network (Scheme 2a). For the 1:1 complexes, the segregated stacks (Scheme 2b) are obtained in **7**, **9**, **12–15**, and **18** and the alternated ones (Scheme 2c) are realized in **8**, **10**, **11**, **16**, and **17**. The molecular tapes in the complexes which gave the segregated stacks are roughly planar, and the dihedral angles between the rings are small. Thus, the favorable overlapping of the tapes causes the segregated stacks. In contrast, the molecular tapes in **8**, **10**, **11**, **16**, and **17** have larger dihedral angles between the rings such as a chain. This steric effect and the favorable charge-transfer interactions between the anilic acids and the dipyrindyl compounds might bring the alternated stacks.



Conclusions

In this study, we have shown that the simple combination of anilic acids and dipyriddy compounds can create a variety of supramolecular architectures by self-assembly. The crystalline architectures described here are composed of an infinite one-dimensional molecular tape structure via the supramolecular synthon **I** with three types of intermolecular hydrogen bonds ($N^+-H\cdots O^-$, $N^+-H\cdots O$, and $O-H\cdots N$). Strong resemblances between the crystal structures of the segregated stacking type (**7**, **9**, **12–15**, and **18**) or the alternated stacking type (**8**, **10**, **11**, **16**, and **17**) suggest the robustness and reproducing ability of the supramolecular synthon **I**. Charge-assistance effect¹⁸ enhances the robustness of the synthon **I** in this system. The positions of the nitrogen atoms of the dipyriddy compounds strongly affect the crystalline architecture and ionicity of the component molecules which can be determined by proton transfer.

Although the anilic acids are well-known to form coordination bonds with a variety of metals,^{14d,15a,b,19} they have not been well exploited for the rational design of organic solids.²⁰ This is the first example in which the anilic acids were used to create the supramolecular synthon **I** for crystal engineering purposes. The combination of two-component systems reported here may be a fundamental example for the design of low-dimensional structures. As an extension of our results, combination of other bidentate nitrogen ligands with proton donors would lead to an interesting crystalline architecture through a supramolecular synthon like **I**. Unusual physical properties such as conductivities may arise from charge-transfer interactions between component molecules.

Experimental Section

Starting Materials. Compounds **1d**,^{7b} **4a**,²¹ **4b**,²² and **4c**²³ were prepared according to the literature methods. Other compounds, **1a–c**, **2**, and **3**, were commercially available and purified by usual methods. All the solvents were distilled before the use for the reactions.

General Procedures for the Preparation of Single Crystals. Method I. An equivalent molar amount (0.03–0.10 mmol) of the anilic acid and the dipyriddy compound was placed

at the bottom of the H-shaped tube, and the tube was filled with solvents (10–25 mL). After 3–30 days, crystals grew at room temperature.

Method II. A solution of the anilic acid (0.05–0.10 mmol) in a freshly distilled hot solvent (5–15 mL) was mixed with a solution of the dipyriddy compound (0.05–0.10 mmol) in a distilled hot solvent (5–10 mL). Within a week, the crystals suitable for single-crystal X-ray diffraction appeared in the flask.

Method III. A solution of the anilic acid (0.05–0.10 mmol) in 10–20 mL of a dry solvent was added to a solution of the dipyriddy compound (0.05–0.10 mmol) in 10–15 mL of a dry solvent. Slow evaporation at room temperature for 1–3 days afforded the colored solution. The single crystals suitable for single-crystal X-ray diffraction were grown from this solution by complete or partial evaporation of the solvent from the reaction mixture. The crystals were characterized by IR, elemental analysis, and X-ray crystallographic analysis.

Complex 5. Red prismatic crystals were prepared from the mixture of acetone–methanol by method I in 96% yield; mp 201–202 °C; IR (KBr) 2350–2800, 2176 (broad), 1630 (sharp), 1517, 1470 cm^{-1} . Anal. Calcd for $C_{26}H_{18}N_4O_4Br_2$ (1:2): C, 51.17; H, 2.97; N, 9.18. Found: C, 51.09; H, 3.02; N, 8.98.

Complex 6. Red prismatic crystals were prepared from methanol and acetone by method I in 98% yield; mp 214–215 °C; IR (KBr) 2350–2800, 2176 (broad), 1630 (sharp), 1519, 1476 cm^{-1} . Anal. Calcd for $C_{26}H_{18}N_4O_4Cl_2$ (1:2): C, 59.90; H, 3.48; N, 10.75. Found: C, 59.86; H, 3.43; N, 10.70.

Complex 7. Orange plate crystals were prepared from acetone by method II in 90% yield; mp 164–165 °C; IR (KBr) 2360 (broad), 1637, 1601 cm^{-1} . Anal. Calcd for $C_{16}H_{12}N_2O_4$ (1:1): C, 64.86; H, 4.08; N, 9.45. Found: C, 64.67; H, 4.17; N, 9.28.

Complex 8. Brown needle crystals were prepared from acetone by method I in 98% yield; mp 228 °C dec; IR (KBr) 2400–2800, 2170 (broad), 1632 (sharp), 1504, 1488 cm^{-1} . Elemental analysis was previously described.¹¹

Complex 9. Brown plate crystals were prepared from acetone–methanol by method I in 95% yield; mp 215–218 °C dec; IR (KBr) 2400–2800, 2124 (broad), 1640 (sharp), 1548, 1523 cm^{-1} . Elemental analysis was previously described.¹¹

Complex 10. Brown rod crystals were prepared from acetone–methanol (2:1) by method I; yield 92%; mp 252–255 °C dec; IR (KBr) 2250–2700, 2132 (broad), 1625 (sharp), 1506 cm^{-1} . Anal. Calcd for $C_{18}H_{12}N_2O_4Br_2$ (1:1): C, 45.03; H, 2.52; N, 5.83. Found: C, 44.99; H, 2.54; N, 5.58.

Complex 11. Reddish brown prismatic crystals were prepared from acetone–methanol (1:1) by method II in 90% yield; mp 280–282 °C dec; IR (KBr) 2250–2700, 2152 (broad), 1624 (sharp), 1494 cm^{-1} . Anal. Calcd for $C_{18}H_{12}N_2O_4Cl_2$ (1:1): C, 55.26; H, 3.09; N, 7.16. Found: C, 55.18; H, 3.08; N, 7.05.

Complex 12. Orange rod crystals were prepared from acetonitrile–ethanol by method III in 84% yield; mp 195–196 °C; IR (KBr) 2354 (broad), 1648, 1618, 1607 cm^{-1} . Anal. Calcd for $C_{18}H_{12}N_2O_4$ (1:1): C, 67.50; H, 3.78; N, 8.75. Found: C, 67.04; H, 3.84; N, 8.68.

Complex 13. Brown needle crystals were prepared from acetone by method I in 92% yield; mp 190–192 °C; IR (KBr) 2473 (broad), 1660, 1601 cm^{-1} . Anal. Calcd for $C_{18}H_{10}N_2O_4Br_2$ (1:1): C, 42.22; H, 2.11; N, 5.86. Found: C, 44.96; H, 1.92; N, 5.77.

Complex 14. Brown needle crystals were prepared from methanol–acetone (1:1) by method I in 83% yield; mp 194–

(18) Braga, D.; Grepioni, F. *Acc. Chem. Res.* **2000**, *33*, 601.

(19) (a) Calvo, M. A.; Lanfredi, A. M. M.; Oro, L. A.; Pinillos, M. T.; Tejel, C.; Tiripicchio, A.; Ugozzoli, F. *Inorg. Chem.* **1993**, *32*, 1147. (b) Kawata, S.; Kitagawa, S.; Furuchi, I.; Munakata, M. *Angew. Chem., Int. Ed. Engl.* **1994**, *33*, 1759. (c) Kawata, S.; Kitagawa, S.; Kondo, M.; Katada, M. *Synth. Met.* **1995**, *71*, 1917. (d) Decurtins, S.; Schmalke, H. W.; Zheng, L.-M.; Ensling, J. *Inorg. Chim. Acta* **1996**, *224*, 165. (e) Cueto, S.; Straumann, H.-P.; Rys, P.; Petter, W.; Gramlich, V.; Rys, F. *Z. Acta Crystallogr., Sect. C* **1992**, *48*, 458.

(20) (a) Tomura, M.; Yamashita, Y. *CrystEngComm* **2000**, *16*. (b) Ishida, H.; Kashino, S. *Acta Crystallogr., Sect. C* **1999**, *55*, 1149. (c) Ishida, H.; Kashino, S. *Acta Crystallogr., Sect. C* **1999**, *55*, 1714.

(21) Teitei, T.; Collin, P. J.; Sasse, W. H. F. *Aust. J. Chem.* **1972**, *25*, 171.

(22) Teitei, T.; Wells, D.; Sasse, W. H. F. *Aust. J. Chem.* **1973**, *26*, 2129.

(23) Tanner, M.; Ludi, A. *Chimica* **1980**, *34*, 23.

195 °C; IR (KBr) 2484 (broad), 1660, 1607 cm⁻¹. Elemental analysis was previously described.¹²

Complex 15. Brown plate crystals were prepared from acetone by method I in 93% yield; mp 176–178 °C; IR (KBr) 2484 (broad), 1660, 1607 cm⁻¹. Elemental analysis was previously described.¹²

Complex 16. Brown plate crystals were prepared from acetonitrile–acetone (1:4) by method I in 98% yield; mp 218–220 °C; IR (KBr) 2280–2650, 2164, 2081, 1630, 1601, 1520 cm⁻¹. Anal. Calcd for C₁₈H₁₀N₂O₄Br₂ (1:1): C, 45.22; H, 2.11; N, 5.86. Found: C, 45.11; H, 2.11; N, 5.42.

Complex 17. Brown needle crystals were prepared from acetonitrile–acetone (1:1) by method I in 90% yield; mp 230–231 °C; IR (KBr) 2280–2650, 2156, 2062, 1625, 1500 cm⁻¹. Elemental analysis was previously described.¹²

Complex 18. Yellow needle crystals were prepared from acetonitrile by method II in 82% yield; mp >330 °C; IR (KBr) 2350–2880, 2203 (strong), 1632, 1543 cm⁻¹. Anal. Calcd for C₂₀H₁₀N₄O₄ (1:1): C, 63.69; H, 2.82; N, 15.64. Found: C, 64.01; H, 2.89; N, 15.42.

X-ray Crystallography. Reflection data were collected on a Rigaku AFC-7R diffractometer using Mo K α radiation (λ = 0.710 69 Å) and Enraf-Nonius CAD4 diffractometer using Cu K α radiation (λ = 1.541 78 Å) at 296 K. No absorption correction was applied for all crystals except the complexes **13** and **16**. Absorption correction was applied to **13** and **16** using empirical procedures based on azimuthal ψ scans of seven reflections having an Eulerian angle, χ , near 90°. All structures were solved by direct methods and refined by full-matrix least-squares on F^2 with SHELX-97.²⁴ All non-hydrogen atoms were refined anisotropically. All hydrogen atoms were localized in the Fourier maps and refined isotropically.

Crystal data for 5: C₂₆H₁₈Br₂N₄O₄, fw = 610.26, monoclinic, space group $P2_1/n$, a = 8.827(1) Å, b = 11.838(1) Å, c = 11.191(1) Å, β = 92.62(8)°, V = 1168.1(2) Å³, Z = 2, D_c = 1.735 g cm⁻³, $F(000)$ = 608, μ (Cu K α) = 4.770 mm⁻¹, crystal dimensions = 0.20 × 0.20 × 0.20 mm³, 2545 reflections collected, 2391 independent (R_{int} = 0.0356), R_1 = 0.0349, wR_2 = 0.0956 for $I > 2\sigma(I)$, R_1 = 0.0389, wR_2 = 0.0990, S = 1.069 for all data.

Crystal data for 6: C₂₆H₁₈Cl₂N₄O₄, fw = 521.34, monoclinic, space group $P2_1/n$, a = 8.6979(5) Å, b = 11.5377(6) Å, c = 11.2992(6) Å, β = 91.274(4)°, V = 1133.6(1) Å³, Z = 2, D_c = 1.527 g cm⁻³, $F(000)$ = 536, μ (Cu K α) = 2.953 mm⁻¹, crystal dimensions = 0.25 × 0.10 × 0.10 mm³, 2456 reflections collected, 2302 independent (R_{int} = 0.0222), R_1 = 0.0353, wR_2 = 0.0869 for $I > 2\sigma(I)$, R_1 = 0.0701, wR_2 = 0.1004, S = 0.998 for all data.

Crystal data for 7: C₁₆H₁₂N₂O₄, fw = 296.28, monoclinic, space group $C2/c$, a = 20.773(3) Å, b = 7.1001(7) Å, c = 9.157(1) Å, β = 93.355(7)°, V = 1348.3(3) Å³, Z = 4, D_c = 1.460 g cm⁻³, $F(000)$ = 616, μ (Cu K α) = 0.892 mm⁻¹, crystal dimensions = 0.25 × 0.10 × 0.02 mm³, 1184 reflections collected, 1150 independent (R_{int} = 0.1124), R_1 = 0.0612, wR_2 = 0.1267 for $I > 2\sigma(I)$, R_1 = 0.2132, wR_2 = 0.1859, S = 0.982 for all data.

Crystal data for 10: C₁₈H₁₂Br₂N₂O₄, fw = 480.12, monoclinic, space group $P2_1/c$, a = 8.3546(5) Å, b = 8.0001(6) Å, c =

13.261(1) Å, β = 104.495(6)°, V = 858.1(1) Å³, Z = 2, D_c = 1.858 g cm⁻³, $F(000)$ = 472, μ (Cu K α) = 1.858 mm⁻¹, crystal dimensions = 0.10 × 0.10 × 0.10 mm³, 1868 reflections collected, 1750 independent (R_{int} = 0.0202), R_1 = 0.0341, wR_2 = 0.0903 for $I > 2\sigma(I)$, R_1 = 0.0523, wR_2 = 0.1034, S = 0.870 for all data.

Crystal data for 11: C₁₈H₁₂Cl₂N₂O₄, fw = 391.20, monoclinic, space group $P2_1/c$, a = 8.3843(5) Å, b = 7.8904(6) Å, c = 12.926(3) Å, β = 105.033(7)°, V = 825.8(2) Å³, Z = 2, D_c = 1.573 g cm⁻³, $F(000)$ = 400, μ (Cu K α) = 3.794 mm⁻¹, crystal dimensions = 0.10 × 0.10 × 0.02 mm³, 1762 reflections collected, 1683 independent (R_{int} = 0.0492), R_1 = 0.0463, wR_2 = 0.1236 for $I > 2\sigma(I)$, R_1 = 0.1204, wR_2 = 0.1689, S = 0.818 for all data.

Crystal data for 12: C₁₈H₁₂N₂O₄, fw = 320.30, monoclinic, space group $P2_1/n$, a = 3.815(2) Å, b = 10.594(2) Å, c = 18.393(1) Å, β = 95.49(2)°, V = 740.0(4) Å³, Z = 2, D_c = 1.438 g cm⁻³, $F(000)$ = 332, μ (Mo K α) = 0.104 mm⁻¹, crystal dimensions = 0.20 × 0.10 × 0.03 mm³, 1529 reflections collected, 1352 independent (R_{int} = 0.0255), R_1 = 0.0472, wR_2 = 0.1088 for $I > 2\sigma(I)$, R_1 = 0.1238, wR_2 = 0.1280, S = 0.924 for all data.

Crystal data for 13: C₁₈H₁₀Br₂N₂O₄, fw = 478.10, triclinic, space group $P\bar{1}$, a = 3.9452(2) Å, b = 11.0548(4) Å, c = 11.0525(3) Å, α = 60.946(2)°, β = 95.49(2)°, γ = 84.022(3)°, V = 419.04(3) Å³, Z = 1, D_c = 1.895 g cm⁻³, $F(000)$ = 234, μ (Cu K α) = 1.895 mm⁻¹, crystal dimensions = 0.35 × 0.10 × 0.02 mm³, 1781 reflections collected, 1691 independent (R_{int} = 0.0141), R_1 = 0.0320, wR_2 = 0.0869 for $I > 2\sigma(I)$, R_1 = 0.0350, wR_2 = 0.0892, S = 1.015 for all data.

Crystal data for 16: C₁₈H₁₀Br₂N₂O₄, fw = 478.10, monoclinic, space group $P2_1/n$, a = 13.211(1) Å, b = 6.8099(8) Å, c = 18.895(2) Å, β = 95.49(2)°, V = 1696.5(3) Å³, Z = 4, D_c = 1.872 g cm⁻³, $F(000)$ = 936, μ (Cu K α) = 6.316 mm⁻¹, crystal dimensions = 0.20 × 0.15 × 0.05 mm³, 3565 reflections collected, 3459 independent (R_{int} = 0.0183), R_1 = 0.0368, wR_2 = 0.0986 for $I > 2\sigma(I)$, R_1 = 0.0587, wR_2 = 0.1113, S = 0.931 for all data.

Crystal data for 18: C₂₀H₁₀N₄O₄, fw = 370.32, triclinic, space group $P\bar{1}$, a = 8.910(7) Å, b = 9.827(14) Å, c = 5.323(6) Å, α = 102.71(14)°, β = 104.88(9)°, γ = 104.66(12)°, V = 415.0(8) Å³, Z = 1, D_c = 1.482 g cm⁻³, $F(000)$ = 190, μ (Mo K α) = 0.107 mm⁻¹, crystal dimensions = 0.30 × 0.20 × 0.02 mm³, 1620 reflections collected, 1516 independent (R_{int} = 0.1135), R_1 = 0.0584, wR_2 = 0.1150 for $I > 2\sigma(I)$, R_1 = 0.3699, wR_2 = 0.1880, S = 0.890 for all data.

Acknowledgment. We thank Professor K. Nakasuji, Dr. J. Toyoda, and Dr. Y. Morita of Osaka University for their continuous encouragement and advice for this work. M.B.Z. thanks the Institute for Molecular Science for postdoctoral fellowships. This work was supported by a Grant-in-Aid for Scientific Research from the Ministry of Education, Culture, Sports, Science and Technology, Japan.

Supporting Information Available: The X-ray crystallographic data (ORTEP drawings and tables of the crystal data, bond lengths and angles, atomic coordinates, and anisotropic thermal parameters) for **5–7**, **10–13**, **16**, and **18**. This material is available via the Internet at <http://pubs.acs.org>.

JO001746I

(24) Sheldrick, G. M., *SHELX-97. Program for the Solution and the Refinement of Crystal Structures*; University of Göttingen: Göttingen, Germany, 1997.